ISBN: 978-3-95450-184-7 doi:10.18429/JACoW-IPAC2018-TUPAF046

CONCEPTUAL DESIGN OF A COLLIMATION SYSTEM FOR THE CERN SUPER PROTON SYNCHROTRON

M. Patecki*, A. Mereghetti, D. Mirarchi and S. Redaelli, CERN, Geneva, Switzerland

Abstract

The Super Proton Synchrotron (SPS) is the last accelerator in the LHC Injectors Chain. Its performance is constantly being improved in frame of the LHC Injectors Upgrade (LIU) Project in order to prepare it for the future HL-LHC (High Luminosity LHC) operation. One of the LIU goals is to nearly double the intensity extracted from the SPS, up to 2.32×10^{11} p/bunch. In recent years, nearly 10% of losses are observed for nominal intensity and LHC-type beams; they grow to about 20% for the intensity approaching the HL-LHC target. Beam losses imply activation and aging of the SPS hardware; the possibility to add a collimation system is being considered to mitigate this problem.

In this paper we present studies of a collimation system design for the SPS. The concept is based on a primary horizontal collimator located in an available position with high enough dispersion, and a secondary collimator to intercept the particles leaking out from the primary collimator. Performance of the proposed collimation system is evaluated by means of numerical simulations.

INTRODUCTION

The SPS currently delivers to the LHC up to four batches of 72 bunches, accelerated from 26 GeV/c up to 450 GeV/c, with an intensity of about 1.33×10^{11} protons per bunch. The SPS bunch intensity at injection will be nearly doubled (up to 2.57×10^{11} p/b) in the future HL-LHC operation with a budget for particle losses of 10% to guarantee 2.32×10^{11} p/b at extraction.

The beam loss mechanism in the SPS has been extensively studied in the recent years and summarized at the SPS Injection Losses Review held in November 2017 [1]. It was concluded that longitudinal effects are mostly responsible for the observed losses. The main sources of losses are the uncaptured beam from the Proton Synchrotron (PS) due to its longitudinal emittance and tails (S-shape), and particles being close to the separatrix that fall out of the SPS rf bucket. Losses occur mainly in the horizontal plane, at locations of large horizontal dispersion (Fig. 1). The dispersion function changes between the 3 optics being used in the SPS: Q26, Q22 and Q20, denoting the integer value of tune. Beam Loss Monitor (BLM) data [2] indicate that losses are localized in a few locations along the ring rather than equally distributed. This leads to an increased activation, faster aging and potential damage of the machine equipment, especially with an increased intensity of the future HL-LHC beams. Adding an off-momentum collimation system is a potential solution to contain losses in the ring. The objectives for the SPS collimation system are to provide a passive protection against the off-momentum losses and to concentrate the losses in the designed, safe locations. The minimal openings described in the following section must be respected and the collimators must fit into the existing empty slots along the ring.

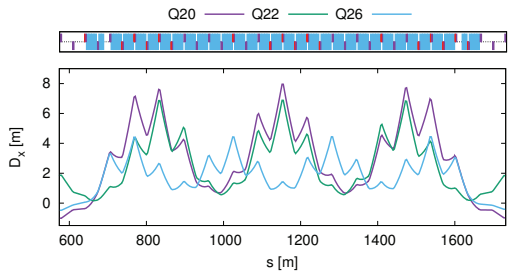

Figure 1: Horizontal dispersion (D_x) for Q20, Q22 and Q26 optics. Only 1/6 of the SPS ring is given due to the optics symmetry. Machine elements are indicated in the top panel: dipoles in blue and quadrupoles in purple.

SPS BEAMS AND DESIGN CONSTRAINTS

The SPS provides beams not only to the LHC, but also to the fixed target (FT) experiments in the North Area or facilities like AWAKE [3] and HiRadMat [4]. The beam parameters (Table 1) and the machine settings can change drastically from cycle to cycle. For any beam, we define a minimum opening of the primary collimator as $4\sigma_\beta + D_x\delta_{p,bh}$, where σ_β is the betatron amplitude and $\delta_{p,bh}$ is the bucket height. Additionally, a large geometrical emittance in the FT case at injection energy results in a large horizontal beam size of up to about 40 mm. Similar extension of the FT beam is reached during the slow extraction process based on the third order resonance [5]. Any collimators added to the SPS ring should stand clear of the FT beam envelope in order to avoid generating unwanted beam losses. Adjusting the collimators gaps between cycles could potentially overcome this limitation, but it can be mechanically challenging. Therefore, in this first study we decided to consider only locations for the collimators compatible with any SPS optics, which are the regions with a high dispersion. Alternatively, the difference between the optimal collimator openings and actual gaps can be compensated by using orbit bumps.

SIMULATION SETUP

Performance of the studied solutions was evaluated by using the coupling [6] between FLUKA [7, 8] and SixTrack [9, 10], where the former simulates the interaction of particles with matter and the latter tracks particles through the machine model in a symplectic manner. Simulations start at the front face of the primary collimator, with 100000

* mpatecki@cern.ch

ISBN: 978-3-95450-184-7 doi:10.18429/JACoW-IPAC2018-TUPAF046

Table 1: Relevant parameters of HL-LHC and fixed target beams in the SPS. E stands for the beam energy and $\varepsilon_{\mathrm{norm;x}}$ for the normalized horizontal emittance.

	E inj./extr. [GeV]	p$^+$/batch [10^{13}]	$\varepsilon_{\mathrm{norm;x}}$ [μm]	optics
HL-LHC	26/450	7.0	1.9	Q20/Q22
FT	14/400	5.9	8 – 12	Q26

particles hitting the inner collimator jaw with an average impact parameter of $0.1 \pm 0.01\mu$m. To correctly reproduce the beam halo distribution, particles horizontal position and angle are defined by randomly assigning a betatron amplitude following a double-Gaussian distribution (90% $1\sigma_{\beta_x}$ and 10% $3\sigma_{\beta_x}$) and adding the required δ_p value to reach the desired extension due to the dispersion. Vertical position and angle follow a Gaussian distribution.

Contrary to a superconducting machine like the LHC, where the peak losses must remain below the quench limits, no immediate limit apply to the peak losses in a machine like the SPS. Instead, the integrated losses represent the concern. FLUKA simulations are done (see [11,12]) in order to assess whether the dose and activation levels are within the acceptable limits. It is of course desirable to keep the amount of aperture losses as low as possible. As discussed at the SPS Injection Losses Review [1], a collimation system reaching a global cleaning efficiency (losses in the collimators divided by the sum of losses in the collimators and in the aperture) of at least 80% with local losses not larger than a few % will provide a sufficient cleaning.

COLLIMATION SYSTEM DESIGN

A first, preliminary concept of the SPS collimation system has been presented already in 2016 [13]. It is based on one primary and one secondary collimator per plane, with primaries located in the first dispersion suppressor of the long straight section 1 (LSS1) and secondaries in the LSS1. This design is characterized by an efficiency of more than 70%, but it has not been further developed as it does not comply with the FT beam requirements and would require adjusting the collimator gaps between cycles [2].

Collimators in the Arc

We propose a compact design of the collimation system, based on both primary and secondary horizontal collimators located in the short straight section (140 cm) of the first arc at the maximum of the last dispersion wave, see Fig. 2. The primary collimator is a 5 mm graphite block located directly downstream of a 60 cm to 1 m long secondary collimator (absorber). The considered materials for the secondary collimator are: molybdenum-graphite (MoGr) [14], copper (Cu) or tungsten (W). Opening of the primary collimator is set to $4\sigma_{\beta_x} + D_x\delta_{p,bh}$ (39.1 mm, Q20) and $1\sigma_{\beta_x}$ retraction is added to the secondary collimator (41.6 mm, Q20). Same openings can be used also for the Q22. Such an unusual configuration has been chosen to better use the little space

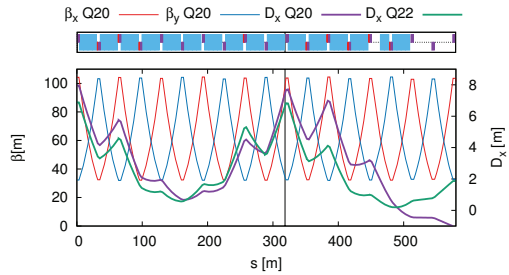

Figure 2: Location of collimation insertion (a black vertical line) w.r.t. the optical functions. β in Q22 optics is nearly the same as in Q20 optics.

available. A role of the short primary collimator is to cause an energy loss and betatron amplitude growth, both small enough to let the particles hit the front face of the secondary collimator at subsequent turns without being lost in the aperture. This allows for profiting from the whole length of the absorber. Without the primary collimator, most particles would interact only with the end part of the absorber, leading to a poor performance.

The collimation efficiency reaches 73% for an absorber made of 1 m of MoGr and grows to 85% and 88% when using 1 m of Cu or 60 cm of W, respectively. This means that 1 m of MoGr is not enough to stop all the secondary halo, which is the case for the considered absorbers made of Cu and W. The cleaning inefficiency plots (so-called loss maps) for a MoGr case are given in Fig. 3. The loss map over the entire length of the machine shows that most of the losses occur at the collimators with a few small localized aperture losses still being present. A zoom into the region directly downstream of the collimators shows that this location is the most exposed to secondary halo particles leaking out from the collimators. A detailed energy deposition study [11] showed that the downstream elements will receive a dose of about a MGy/year, allowing for at least 25-30 years of operation. Tight space conditions do not allow for installing any efficient shielding. The energy deposited in the collimators will cause a temperature raise per beam train of some tens of K (absorber, MoGr and Cu) to some hundreds of K (primary collimator, absorber W). A material activation study shows that the collimators region may become significantly activated [12], which can be mitigated by shielding the affected elements. We conclude that the secondary showers do not set any limitation for such a collimation system, however, they must be handled carefully.

The aforementioned results refer to the Q20 optics but the conclusions are expected to hold also for Q22 optics, for which a few % higher collimation efficiency is observed.

Absorber in the LSS1

Fitting both collimators into the arc is challenging due to the space constraints and leads to an unavoidable irradiation of the downstream elements. These disadvantages can be solved by moving the absorber two cells downstream, to the

ISBN: 978-3-95450-184-7 doi:10.18429/JACoW-IPAC2018-TUPAF046

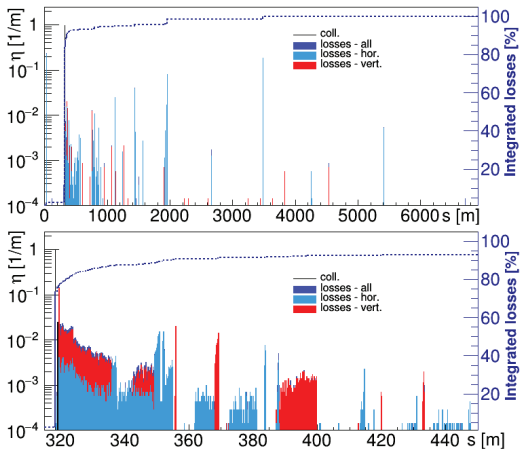

Figure 3: Loss maps for 1 m MoGr absorber, Q20. Top: entire ring. Bottom: region downstream of the collimators.

dispersion suppressor region, upstream of the TIDP [15]. The TIDP is an old momentum collimator, used with Q26 optics. Its core is composed of 1.6 m of aluminium followed by 2.5 m of copper, with a horizontal aperture of 41 mm on the inner side of the ring. The core is surrounded by a 4.3 m long iron tank. In this configuration, a primary collimator is moved one cell downstream (see Fig. 4) to set a phase advance closer to 90°. In fact, the betatron amplitude increase is more relevant in this scenario as the dispersion at the absorber is much smaller, see Fig. 4. The opening of the primary collimator follows the condition $4\sigma_{\beta_x} + D_x\delta_{p,bh}$ which results in gaps of 36.1 mm (Q20) and 26.2 mm (Q22), both fulfilling the FT beam requirements. An efficient cleaning is obtained for the absorber gap set to $5\sigma_{\beta_x} + D_x\delta_{p,bh}$ which corresponds to 24.8 mm (Q20) and 16.9 mm (Q22), but violates the minimum opening requirement of the FT beam. Enough beam clearance is achieved if the absorber gap is increased to about 41 mm and a local, 3-correctors orbit bump is used to reach the absorber. The selected orbit correctors are MDH.11207 (just downstream of the primary collimator), MDH.11407 (just upstream of the absorber) and MDH.11605. This allows creating an orbit bump that opens downstream of the primary collimator, reaches a maximum extension ($\leq$ 25 mm) at the absorber and closes immediately after. In case of 1 m long MoGr absorber upstream of the

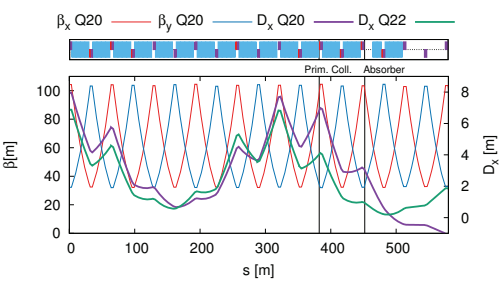

Figure 4: Location of collimators (black vertical lines) w.r.t. the optical functions. β in Q22 nearly the same as in Q20.

TIDP, the cleaning efficiency reaches 87% for Q20 optics and 84% for Q22 optics with the TIDP contributing by 8% in both cases. If the TIDP is the only absorber, the cleaning efficiency reaches 82% for Q20 and 80% for Q22. It is worth to mention that local aperture losses are much lower compared to the scenario with collimators in the arc. An example of loss map for Q20 optics is given in Fig. 5, a better cleaning performance is visible. There is also enough space to insert additional shielding, if needed. The energy deposition and activation studies are in progress for this scenario.

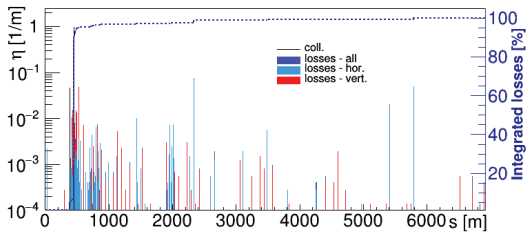

Figure 5: Loss maps for 1 m long MoGr absorber located upstream of the TIDP, Q20 optics.

Alternatively, an absorber at 41 mm can be reached by using a bent crystal as a primary collimator with a deflection angle of about 300 μrad. It avoids using the orbit bump, but requires a very precise control over the crystal angular orientation, to several μrad. Such a design is currently under investigation.

CONCLUSIONS AND OUTLOOK

An off-momentum collimation system can be a viable solution to the beam losses in the SPS expected with HL-LHC beams. Two designs have been proposed, both considering a two-stages collimation system. The first design conceives both stages in the arc, at the peak of dispersion. It makes the system very compact and insensitive to the common machine errors, providing a good cleaning efficiency. The second design conceives to move the second stage to the dispersion suppressor region and therefore reduce the radiation effects on the elements immediately downstream. This design is characterized by an improved cleaning efficiency, but it requires a well controlled orbit bump. It also allows to use the TIDP as a secondary stage, with no substantial degradation of the cleaning performance.

It is planned to compare in detail the two options based on energy deposition studies, feasibility of the orbit bump control and robustness to errors. Decision on the collimation system implementation is expected by the end of 2018.

ACKNOWLEDGEMENT

Many thanks to V. Kain and H. Bartosik for providing input on beam losses and feedback on various proposals, to M. Fraser, L. Stoel and F. Velotti for explaining the details of the FT beam, to L. Salvatore and D. Björkman for energy deposition and activation studies, and to the LIU SPS Beam Loss, Protection, Transfer Lines (BLPTL) Working Group members for useful comments and discussions.

ISBN: 978-3-95450-184-7 doi:10.18429/JACoW-IPAC2018-TUPAF046

REFERENCES

[1] SPS Injection Losses Review 2017, https://indico.cern.ch/event/672967/

[2] M. Patecki, A. Mereghetti, D. Mirarchi and S. Redaelli, *Conceptual design of the SPS collimation system*, SPS Injection Losses Review 2017, https://indico.cern.ch/event/672967/contributions/2789731/

[3] C. Bracco et al., *AWAKE: a Proton Driven Plasma Wakefield Acceleration Experiment at CERN*, ICHEP 2016.

[4] Efthymiopoulos et al., *HiRadMat: a New Irradiation Facility for Material Testing at CERN*, IPAC 2011.

[5] F. M. Velotti et al., *Characterisation of the SPS Slow-Extraction Parameters*, IPAC 2016.

[6] R. Bruce et al., *Status of Fluka coupling to Sixtrack*, in proceedings of Tracking for Collimation Workshop (WP5), CERN, Geneva, Switzerland, in publication.

[7] A. Fasso et al., *FLUKA: a Multi-Particle Transport Code*, CERN-2005-10, INFN/TC-05/11, SLAC-R-773.

[8] G. Battistoni et al., *The FLUKA code: description and benchmarking*, Hadronic Shower Simulation Workshop 2006.

[9] G. Ripken and F. Schmidt, *A Symplectic Six-Dimensional Thin-Lens Formalism for Tracking*, DESY 95-63 and CERN/SL/95-12(AP), 1995

[10] http://sixtrack.web.cern.ch

[11] L. Esposito, *FLUKA studies of the SPS off-momentum collimation system: scraper + absorber*, LIU-SPS BLPTL WG Meeting 7.2.2018, https://indico.cern.ch/event/702596/contributions/2881763/

[12] D. Björkman, *RP Scraper geometry study*, LIU-SPS BLPTL WG Meeting 14.3.2018, https://indico.cern.ch/event/709787/contributions/2916216/

[13] D. Mirarchi et al., *SPS collimation first look and ideas*, LIU-SPS BLPTL WG Meeting 23.3.2016, https://indico.cern.ch/event/510084/contributions/2032084/

[14] O. Sacristan de Frutos et al., *Thermo-Physical and Mechanical Characterisation of Novel Materials under Development for HL-LHC Beam Intercepting Devices*, IPAC 2017.

[15] M. Calviani, *Review of SPS beam intercepting devices*, SPS Losses and Avtivation WG Meeting 22.2.2017, https://indico.cern.ch/event/614375/contributions/2477457